PROCEEDINGS OF SPIE

SPIEDigitalLibrary.org/conference-proceedings-of-spie

Multimode input for dissipative sensing enhancement in whispering-gallery microresonators

Rajagopal, Sreekul Raj, Sandoval, Karleyda, Rosenberger, A. T.

Sreekul Raj Rajagopal, Karleyda Sandoval, A. T. Rosenberger, "Multimode input for dissipative sensing enhancement in whispering-gallery microresonators," Proc. SPIE 11700, Optical and Quantum Sensing and Precision Metrology, 117002T (5 March 2021); doi: 10.1117/12.2586673

SPIE.

Event: SPIE OPTO, 2021, Online Only

Multimode input for dissipative sensing enhancement in whispering-gallery microresonators

Sreekul Raj Rajagopal, Karleyda Sandoval, and A. T. Rosenberger*
Department of Physics, Oklahoma State University, Stillwater, OK, USA 74078-3072

ABSTRACT

Optical whispering-gallery mode (WGM) microresonators have been widely used as chemical sensors. In practice, most WGM sensing is based on either mode frequency shift (dispersive) or mode linewidth change (dissipative). However, WGM sensors based on the fractional change in throughput dip depth (dissipative) can offer better sensitivity under certain conditions. Recently it was demonstrated that for WGM dip-depth sensors multimode input can further improve the sensitivity as compared to single-mode input. This enhancement in sensitivity is achieved by using an asymmetric tapered fiber to couple light in and out of the microresonator. In this report, we develop a model which predicts the waist radius of the fabricated asymmetric tapered fiber. The radius predicted by the model is verified by measuring the beat length for the two fiber modes that are excited and couple into a WGM.

Keywords: microresonator, whispering-gallery modes, multimode input, dissipative sensing, asymmetric tapered fibers.

1. INTRODUCTION

Over the past few decades, optical whispering gallery mode (WGM) microresonators with high quality factors and small mode volumes have emerged as an exceptional platform for various sensing applications.[1] Owing to their high sensitivities and low detection limits, optical sensors based on WGM microresonators have been used to monitor various physical quantities. The sensing technique of an optical WGM sensor can be classified as dispersive or dissipative. Dispersive sensing entails measuring the shift in WGM resonance frequency due to a change in the surrounding medium's refractive index.

In contrast, in general, dissipative sensing relies on measuring the change in WGM linewidth due to absorption in a lossy analyte in the surrounding medium. However, besides the linewidth change, the analyte's absorption also induces a change in the resonant throughput dip depth. Consequently, one can study dissipative sensing by monitoring this change. Previously it was shown that dissipative sensing based on the fractional change in resonant throughput dip depth could provide better sensitivity than dispersive sensing.[2,3] Recently a novel method for enhancing the sensitivity of resonant throughput dip depth based dissipative sensing was proposed[4] and demonstrated.[5]

Tapered optical fibers enable efficient coupling of light into and out of WGMs. In general, fiber tapers can be broadly classified as adiabatic (as our symmetric tapered fiber) or non-adiabatic (as the downtaper of our asymmetric tapered fiber). Recently non-adiabatic tapered fibers have been used for sensing refractive index[6], temperature[7], and magnetic field.[8] Usually, adiabatic tapered fibers are used to excite a single fiber mode for coupling into a WGM, but non-adiabatic tapered fibers can also be used to excite multiple fiber modes for WGM coupling. The work presented in this paper focuses on enhanced chemical absorption sensing using multimode input to a WGM microresonator.

2. SENSING ENHANCEMENT: THEORY AND EXPERIMENT

The behavior of a non-adiabatic tapered fiber-coupled microresonator system was previously demonstrated.[4,5,9] Having multimode input produces an enhancement in the sensitivity of dissipative dip-depth based sensing compared to the sensitivity achieved using single-mode input from a coupling fiber with the same waist radius. The enhancement factor η is given by

*atr@okstate.edu; phone 1 405 744-6742; fax 1 405 744-6811; rosenberger.okstate.edu

Optical and Quantum Sensing and Precision Metrology, edited by Selim M. Shahriar, Jacob Scheuer, Proc. of SPIE Vol. 11700, 117002T · © 2021 SPIE
CCC code: 0277-786X/21/$21 · doi: 10.1117/12.2586673

$$\eta = \left| \frac{1-\frac{1}{2}\left(\sqrt{R_{00}}-\sqrt{R_{0\pi}}\right)}{\sqrt{R_{00}}-\sqrt{R_{0\pi}}} \right| \frac{2\sqrt{R_{00}}}{1-\sqrt{R_{00}}} \simeq \left| \frac{2}{R_{00}-R_{0\pi}} \right| \frac{4}{M_{00}}, \quad (1)$$

where, for the WGM of interest, R_{00} and $R_{0\pi}$ represent the ratios of resonant to off-resonant throughput power when the fiber modes are in and out of phase and M_{00} represents the dip depth $(1-R_{00})$. It is worth noting that η is the ratio of the fractional change in dip depth with multiple modes incident on the microresonator to the fractional change in dip depth with one mode incident on the microresonator. The factor $\frac{4}{M_{00}}$ in Eq. (1) is approximately equal to the ratio of the fractional change in WGM dip depth to the fractional change in WGM linewidth, both for multimode input. Thus, we can compare the dissipative sensing signal based on the relative dip depth change to the signal based on the change in linewidth.

In general, the absolute sensitivity of a tapered fiber coupled microresonator system will depend on the interacting WGM mode fraction *f* and the quality factor *Q* of the WGM. The absolute sensitivity of an asymmetric tapered fiber coupled microresonator system with multiple modes incident on the microresonator is proportional to the product of $\frac{4}{M_{00}}$ and the quality factor *Q*. For an ideal adiabatic tapered fiber coupled microresonator system with a single mode incident on the microresonator, where "ideal" means that the fiber waist radius is not equal to that in the multimode case, but is chosen so that *Q* can be as large as possible, the absolute sensitivity is proportional to (with the same constant of proportionality if *f* is the same) the product of the *intrinsic quality factor* Q_i and $\left|\frac{1-x}{1+x}\right|$, where x represents the ratio of outcoupling loss to the effective intrinsic loss. In order to have equal absolute sensitivity, for the single-mode-incident case there is a minimum intrinsic *Q* required, namely,

$$Q_i \simeq \frac{4}{M_{00}} \left|\frac{1+x}{1-x}\right| Q \geq \frac{4}{M_{00}} Q. \quad (2)$$

For the experiments, we use hollow bottle resonators (HBRs); their use in our lab for internal chemical absorption sensing was previously reported.[10] Light from a tunable diode laser which is scanned in frequency is used to excite the WGMs of an HBR. Initially a non-adiabatic tapered fiber of an arbitrary waist radius was used to couple light into and out of the microresonator. Based on the theory predictions a WGM whose throughput changes from dip to peak, upon translating the point of fiber-HBR contact along the fiber waist, was chosen as the mode of interest. With the fiber modes in phase, predetermined concentrations of analyte (an absorbing dye) were added to the methanol-filled HBR and corresponding dip depths and linewidths were recorded. Then the non-adiabatic tapered fiber was replaced by an adiabatic tapered fiber of the same arbitrary waist radius and the dip depths and linewidths of the same mode corresponding to different analyte concentrations were recorded.

A detailed analysis of finding the experimental enhancement factor from the recorded dip depth was demonstrated in our previous work.[5] A selection of experimental results using different asymmetric tapered fibers is shown in Table 1.

Table 1. Typical experimental results.

Taper profile	R_{00}	$R_{0\pi}$	η - theory	η -experimental	$\frac{4}{M_{00}}$	$(Q_i)_{\min}$
1	0.965	1.073	2135 ± 132	2695 ± 955	114 ± 7	1.6×10^9
2	0.927	1.030	1020 ± 38	956 ± 240	55 ± 2	4.95×10^8
3	0.936	1.040	1166 ± 47	1204 ± 362	62.5 ± 2	6.96×10^8

A sensitivity enhancement of approximately three orders of magnitude was achieved by having multiple modes incident on a microresonator using an asymmetric tapered fiber, compared to the sensitivity using single-mode input from a fiber with the same waist radius. Also, the dip-depth-change sensitivity is shown to be approximately two orders of magnitude greater than the linewidth-change sensitivity. In the ideal case (different waist radius), with one mode incident on the microresonator, to have equal absolute sensitivity as compared to the multimode case the value of Q_i needs to be approximately of the order of 10^9 which is difficult to maintain in fused silica.

3. FABRICATION OF ASYMMETRIC TAPERED FIBERS AND DELINEATION CURVES

In our lab, a homemade fiber puller device using the flame brush technique is used to make both the symmetric adiabatic tapered fibers and asymmetric non-adiabatic tapered fibers. After removal of its jacket, the optical fiber is attached to two motorized translation stages of the fiber puller. Under the stripped portion of the fiber, a hydrogen torch is installed on a third translation stage. When fabricating a symmetric adiabatic tapered fiber, the two stages are pulled at equal speed while the hydrogen flame brushes a fixed length known as the brushing length L. In order to produce an asymmetric tapered fiber with a non-adiabatic downtaper and adiabatic uptaper, the two translation stages are pulled at different speeds for the same time while the hydrogen flame brushing length is usually shorter than in the symmetric case. A schematic diagram of the asymmetric tapered fiber is shown in Fig. 1.

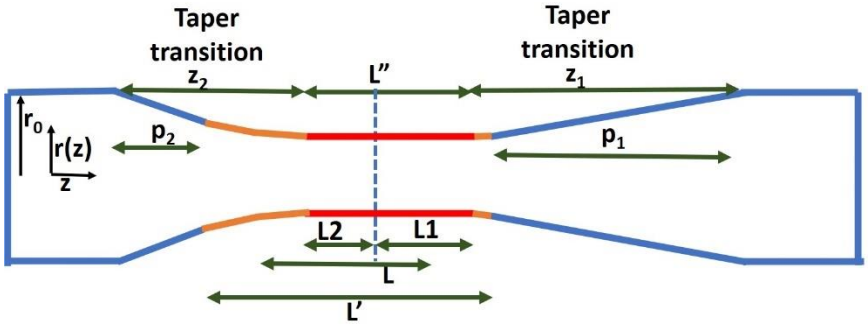

Fig. 1. Asymmetric tapered fiber with non-adiabatic downtaper and adiabatic uptaper. A detailed description is given in Section 4.

For a taper transition to be adiabatic, the cladding taper angle Ω_{cl} must be less than some maximum value[11] at all values of the inverse taper ratio $\frac{r(z)}{r_0}$, where z is the distance from the untapered fiber to the point of interest and $r(z)$ is the local cladding radius with $r_0 = r(0)$. The maximum cladding taper angle for the taper transition to be adiabatic is given by

$$\Omega_{\max} = \frac{r_{cl}}{z_b} = \frac{r_{cl}\left(\beta_f - \beta_h\right)}{2\pi}, \tag{3}$$

where $\beta_f(z)$ and $\beta_h(z)$ are the propagation constants of the fundamental and higher order (family) fiber modes. The propagation constant in a step-index dielectric waveguide is obtained by solving the characteristic equation. The beat length z_b is given by

$$z_b = \frac{2\pi}{\beta_f - \beta_h}. \tag{4}$$

$\Omega_{\max}\left(\frac{r(z)}{r_0}\right)$ thus provides a delineation curve with which the cladding taper angle can be compared to determine the adiabaticity. Knowing the propagation constants at various taper radii allows us to calculate the beat length.

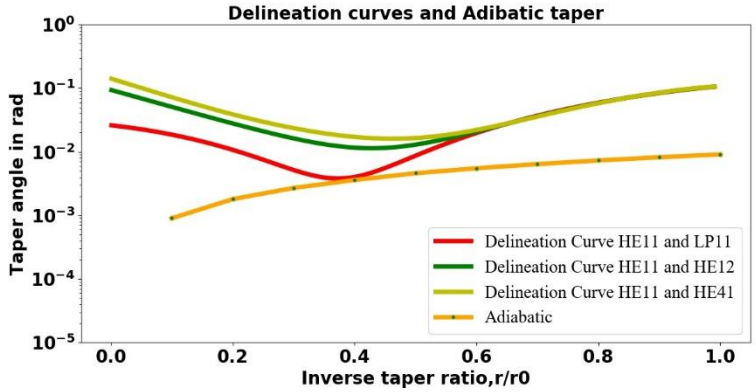

Fig. 2. Delineation curves and the plot of cladding taper angle Ω_{cl} as a function of inverse taper ratio for an adiabatic taper.

For an untapered fiber, the light remains in the fundamental mode (HE_{11}) as the light propagates down the fiber. Upon tapering down to a waist radius of 1.16 μm, in addition to the fundamental mode HE_{11}, other families of modes such as LP_{11} = TE_{01}/TM_{01}/HE_{21}, HE_{12} (plus HE_{31}/EH_{11}), and HE_{41}/EH_{21} can propagate and hence the taper waist is multimode. Thus, while calculating $\Omega_{\max}$ using Eq. (3), β_f will be the propagation constant of the local fundamental HE_{11} mode whereas β_h can be the propagation constant of the higher order modes namely LP_{11}, HE_{12}, and HE_{41}. Since we have three choices for the value of β_h, we will have three delineation curves. In order to plot the delineation curve, the larger of the $\Omega_{\max}$ values for core and cladding guidance at different values of inverse taper ratio was used. These $\Omega_{\max}$ values were fitted to a polynomial and is shown in Fig. 2. The three curves coincide for core guidance because it is single-mode and β_h is simply calculated using the cladding index of refraction.

In Fig. 2, the red, green, and yellow curves represent different delineation curves. The red curve represents the delineation curve plotted by assuming β_h to be the propagation constant of the LP_{11} mode. In contrast, the green and yellow curves represent the delineation curves plotted by assuming β_h to be the propagation constant of HE_{12} and HE_{41} respectively. For all values of inverse taper ratio, an adiabatic taper will have a taper angle Ω_{cl} which is always below the delineation curves (red/green/yellow curves) whereas for a non-adiabatic taper, the plot of the taper angle will pass above the delineation curve for at least some values of the inverse taper ratio. The correct delineation curve is determined by experimental measurement of beat length, as described in the next section. The orange curve represents the taper angle calculated for an adiabatic taper fabricated in our lab.

4. ASYMMETRIC TAPERED FIBER MODEL

A schematic representation of an asymmetric tapered fiber was shown in Fig. 1. The radius of the untapered fiber and brushing length are represented by r_0 and L respectively. Our model is based on the following assumptions:

i. The hydrogen flame has a definite width and hence the heated region L' extends 0.260 mm beyond the flame brush length L on each end.

ii. The end of the uniform waist is not at the end of the limit of the heated region, but inside it by a distance that is inversely proportional to the pulling distance.

Since the fiber is heated and pulled at the same time the limit of the waist is recessed from the end of the heated region by a distance estimated to be $rec = 0.131$ mm for a standard symmetric taper. The length of the uniform waist is given by

$$L'' = L' - rec \times \left(\frac{26.88}{p_1} \right) - rec \times \left(\frac{26.88}{p_2} \right), \tag{5}$$

where p_1 and p_2 represent the pull distances of the two motorized stages; in the symmetric case they are both equal to 26.88 mm. The taper transition lengths on the two sides are given by

$$z_1 = p_1 + rec \times \left(\frac{26.88}{p_1} \right), \tag{6}$$

$$z_2 = p_2 + rec \times \left(\frac{26.88}{p_2} \right). \tag{7}$$

For any tapered fiber, the radius $r(z)$ in the transition region on side *i* can be written as

$$r(z) = r_0 e^{-\frac{z}{2L_i}}, \tag{8}$$

where *z* is the distance into the transition region from the untapered fiber and L_i is the length of the corresponding part of the taper waist ($L_1/L_2 = z_1/z_2$). Thus, the cladding taper angle Ω_{cl} is given by

$$\Omega_{cl}(z) = -\frac{dr(z)}{dz} = \frac{1}{2L_i} r(z). \tag{9}$$

Using the above model, for a given set of parameters $(p_1 = 27.64 \text{ mm}, p_2 = 3.12 \text{ mm}, L = 4.75 \text{ mm})$, a non-adiabatic taper fiber was fabricated, and cladding taper angles were calculated using Eq. (9). The cladding taper angles for the asymmetric tapered fiber (Taper profile 1) with a non-adiabatic downtaper and an adiabatic uptaper were calculated using Eq. (9) and are plotted along with the delineation curves in Fig. 3.

As noted in Section 2 above, the throughput profile of a non-adiabatic tapered fiber coupled microresonator system is no longer a symmetric Lorentzian[12] and it depends on the relative phase of the fiber modes. The beat length was measured by translating the point of fiber-HBR contact along the fiber waist. Upon translating the point of contact, the throughput spectral profile of the non-adiabatic tapered coupled microresonator system changes from a dip to a peak in a periodic manner. The distance the fiber needs to be translated from a peak or dip to the next peak or dip is defined as one beat length. The average beat lengths for three different taper profiles were measured and are shown in Table 2. The measured beat lengths agreed with the calculated ones assuming the higher-order modes were LP_{11} and confirmed the waist radius predicted by the model above. Then the model was used to find the necessary pull distance to fabricate a symmetric tapered fiber of the same waist radius r_w.

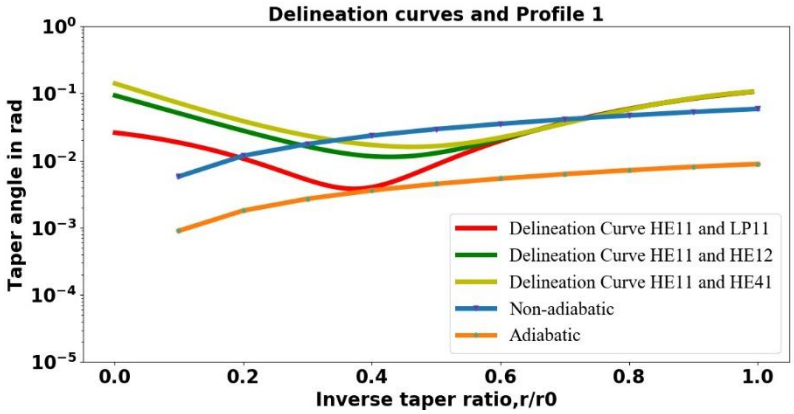

Fig. 3. Delineation curves and the plot of cladding taper angle Ω_{cl} as a function of inverse taper ratio for a non-adiabatic downtaper and adiabatic uptaper.

Table 2. Taper profiles and beat length.

Taper profile	p_1	p_2	L	r_w	Beat length
1	27.64 mm	3.12 mm	4.75 mm	1.16 μm	12.98 μm
2	26.35 mm	3.35 mm	4.78 mm	1.47 μm	20.08 μm
3	28.20 mm	3.45 mm	4.74 mm	1.16 μm	12.76 μm

5. CONCLUSIONS

A model for predicting the radius of the waist of an asymmetric tapered fiber with a non-adiabatic downtaper and an adiabatic uptaper was developed. Based on the model, asymmetric tapered fibers of different taper radii were fabricated, and the beat lengths were measured while being used to couple light in and out of the microresonator. The experimentally measured beat length for the three different profiles suggest that:

i. The modes responsible for beating are HE_{11} and LP_{11} and hence the delineation curve of interest is the red curve shown in Fig. 2 and Fig. 3.
ii. The radii predicted by the asymmetric fiber model for the three different profiles were very close to the estimated radii from the beat length measurements.

The asymmetric tapered fibers of different taper profiles were used in dye absorption sensing experiments. The sensitivities they provided were compared to the sensitivities found using symmetric tapered fibers having the same waist radii, and the results were shown in Table 1.

Dissipative sensing enhancement by using multimode input is not limited to tapered-fiber coupled WGM microresonators. The method can be applied to any waveguide-coupled microresonator sensor.

REFERENCES

[1] Foreman, M. R., Swaim, J. D., and Vollmer, F., "Whispering gallery mode sensors," Adv. Opt. Photon. 7, 168- 240 (2015).

[2] Rosenberger, A. T., "Analysis of whispering-gallery microcavity-enhanced chemical absorption sensors," Opt. Express 15, 12959-12964 (2007).

[3] Farca, G., Shopova, S. I., and Rosenberger, A. T., "Cavity-enhanced laser absorption spectroscopy using microresonator whispering-gallery modes," Opt. Express 15, 17443-17448 (2007).

[4] Rosenberger, A. T., and Rajagopal, S. R., "Enhanced dissipative sensing in a microresonator with multimode input (theory)," Proc. SPIE 11296, 112963D (2020).

[5] Rajagopal, S. R. and Rosenberger, A. T., "Enhanced dissipative sensing in a microresonator with multimode input (experiment)," Proc. SPIE 11296, 112963Q (2020).

[6] Ding, Z., Sun, K., Liu, K., Jiang, J., Yang, D., Yu, Z., Li, J., and Liu, T., "Distributed refractive index sensing based on tapered fibers in optical frequency domain reflectometry," Opt. Express 26, 13042-13054 (2018).

[7] Muhammad, M. Z., Jasim, A. A., Ahmad, H., Arof, H., and Harun, S. W., "Non-adiabatic silica microfiber for strain and temperature sensors," Sensors and Actuators A 192, 130-132 (2013).

[8] Luo, L., Pu, S., Tang, J., Zeng, X., and Lahoubi, M., "Reflective all-fiber magnetic field sensor based on microfiber and magnetic fluid," Opt. Express 23, 18133-18142 (2015).

[9] Rosenberger, A. T., "Absorption sensing enhancement in a microresonator coupled to a non-adiabatic tapered fiber," Proc. SPIE 10548, 105480G (2018).

[10] Stoian, R.-I., Bui, K. V., Rosenberger, A. T., "Silica hollow bottle resonators for use as whispering gallery mode based chemical sensors," J. Opt. 17, 125011 (2015).

[11] Love, J. D., Henry, W. M., Stewart, W. J., Black, R. J., Lacroix, S., and Gonthier, F., "Tapered single-mode fiber devices Part 1: Adiabaticity criteria," IEE Proc.-J: Optoelectron. 138, 355-364 (1991).

[12] Zhang, K., Wang, Y., and Wu, Y.-H., "Enhanced Fano resonance in a non-adiabatic tapered fiber coupled with a microresonator," Opt. Express 42, 2956-2959 (2017).